

ON THE INFLUENCE OF PRESSURE ON THE PHASE EQUILIBRIUM GRAPHITE– CEMENTITE IN THE IRON–CARBON SYSTEM

The transformation

1963

SovietRxiv

View the original and related papers at <https://sovietrxiv.org/items/ru-196301.59007>

Source: Math-Net.Ru and CyberLeninka. Machine translation. Verify with the original.

Abstract

Full Text

PHYSICAL CHEMISTRY

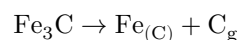
T. P. ERSHOVA, E. G. PONYATOVSKII

**ON THE INFLUENCE OF PRESSURE ON
THE PHASE EQUILIBRIUM GRAPHITE–CE-
MENTITE IN THE IRON–CARBON SYSTEM**

(Presented by Academician G. V. Kurdyumov, March 4, 1963)

The stable diagram for Fe–C alloys in the temperature interval from 0°K to the melting temperature of iron is the Fe–C_g (graphite) diagram. The Fe–Fe₃C (cementite) diagram is metastable. Nevertheless, cementite is one of the principal structural constituents of cast irons and steels and is readily formed not only during phase transformations in the solid state, but also in the process of crystallization of cast irons from the melt under rapid cooling.

The transformation



cementite saturated graphite

with carbon

at atmospheric pressure is accompanied by an increase in volume and by a relatively small decrease in the thermodynamic potential of the system. Consequently, as a result of applying hydrostatic pressure higher than some value definite for the given temperature, cementite will become the stable phase, i.e., the Fe–Fe₃C diagram will become stable, and the Fe–C_g diagram metastable.

In the present work a thermodynamic calculation has been carried out of the temperature dependence of the equilibrium pressure for the transformation $\text{Fe} + \text{C}_g \rightleftharpoons \text{Fe}_3\text{C}$ in the Fe–C system, both for the α - and for the γ -region.

The calculation was carried out on the assumption that 1) the solubility of carbon in α -Fe is equal to zero; 2) the solubility of carbon in γ -Fe does not depend on pressure; 3) the volume effect of the transformation likewise does not depend on pressure.

These assumptions make it possible to write the change in the thermodynamic potential of the system ΔG as a result of the transformation $\text{Fe}_{(\text{C})} + \text{C}_{\text{g}} \rightarrow \text{Fe}_3\text{C}$ at various pressures P and temperatures T in the form

$$\Delta G(T, P) = \Delta G_0(T) + P\Delta V_0(T),$$

where $\Delta G_0(T)$ is the change in thermodynamic potential, and $\Delta V_0(T)$ is the volume effect of the transformation at temperature T and atmospheric pressure, whence the equilibrium pressure P^* at temperature T can be determined as

$$P^*(T) = -\frac{\Delta G_0(T)}{\Delta V_0(T)}.$$

The values of $\Delta G_0(T)$ at different temperatures for the reaction with α -Fe were taken from the works of Richardson ⁽¹⁾, Elliott and Gleiser ⁽²⁾, and Darken and Gurry ⁽³⁾; and for the reaction with $\gamma = \text{Fe}_{(\text{C})}$, saturated with carbon, from work ⁽³⁾.

In determining the values of $\Delta V_0(T)$, the thermal expansion of α -Fe, graphite, and cementite was taken into account, as well as the change in the specific volume of γ - $\text{Fe}_{(\text{C})}$, saturated with carbon, with temperature and composition. The values of the specific volumes and mean coefficients of thermal expansion used in the calculation are given in Table 1. For the value of the specific volume of graphite

the adopted average value, obtained from specific volumes calculated from the most frequently encountered values in the literature for the densities of graphite, equal to 2.25 g/cm³ ^(4,5) and 2.26 g/cm³ ⁽⁶⁻⁸⁾. The volume coefficient of thermal expansion of graphite was calculated from the values of the coefficients of linear expansion along ⁽⁹⁾ and perpendicular to ⁽¹⁰⁾ the hexagonal axis ($\alpha_v = \alpha_{\parallel} + 2\alpha_{\perp}$). The average volume coefficient of thermal expansion of α -Fe was calculated from the temperature dependence of the lattice parameter of α -Fe measured by Basinskii et al. ⁽¹³⁾. The data given in Table 1 on the solubility of carbon in γ -Fe correspond to temperatures of 1000, 1100, 1200, 1300, and 1400°K ⁽³⁾, and the corresponding specific volumes were calculated from the value of the specific volume of pure γ -Fe, equal to 0.12227 cm³/g, and the linear dependence of the density of austenite on carbon content, taken from work ⁽¹²⁾.

Table 1

Phase	Specific volume at 20° C, cm ³ /mol	Average volume coefficient of thermal expansion ×10 ⁶ , deg ⁻¹
Graphite	5.33	33.3
Fe ₃ C	23.23 ⁽¹¹⁾	37.5 ⁽¹²⁾
α -Fe	7.11 ^(4,7)	44

Fig. 1. Diagram of phase equilibrium graphite–cementite: calculated points $\Delta G_0(T)$ taken from works: a –⁽¹⁾, b –⁽²⁾, v –⁽³⁾; experimental points from works: g –⁽¹⁴⁾, d –Radcliffe et al. ⁽¹⁵⁾, e –⁽¹⁶⁾

Figure 1: Fig. 1. Diagram of phase equilibrium graphite–cementite: calculated points $\Delta G_0(T)$ taken from works: a –⁽¹⁾, b –⁽²⁾, v –⁽³⁾; experimental points from works: g –⁽¹⁴⁾, d –Radcliffe et al. ⁽¹⁵⁾, e –⁽¹⁶⁾

Phase	Specific volume at 20° C, cm ³ /mol	Average volume coefficient of thermal expansion ×10 ⁶ , deg ⁻¹
γ -Fe with 0.64% C ⁽³⁾	6.75	70 ⁽¹²⁾
γ -Fe with 0.95% C	6.71	70 ⁽¹²⁾
γ -Fe with 1.27% C	6.67	70 ⁽¹²⁾
γ -Fe with 1.59% C	6.63	70 ⁽¹²⁾
γ -Fe with 1.92% C	6.60	70 ⁽¹²⁾

From the data obtained, the diagram shown in Fig. 1 was constructed; in it, the bold solid lines show the equilibrium curves of graphite and cementite with respect to α -Fe ($C_r \rightleftharpoons Fe_3C$) _{α} and with respect to the solid solution in γ -Fe ($C_r \rightleftharpoons Fe_3C$) _{γ} .

On the basis of the phase rule, the point of intersection of these curves is at the same time also the point of intersection of the curve for the pressure dependence of the eutectoid-transformation temperature $\gamma \rightleftharpoons \alpha + Fe_3C$ and the analogous curve for the eutectoid transformation $\gamma \rightleftharpoons \alpha + C_r$. The latter transformation, although it is the transformation corresponding to the diagram stable at atmospheric pressure, nevertheless is not observed in practice.

Fig. 1. Diagram of the phase equilibrium graphite–cementite: calculated points $\Delta G_0(T)$ taken from works: a –⁽¹⁾, b –⁽²⁾, v –⁽³⁾; experimental points from works: g –⁽¹⁴⁾, d –Radcliffe et al. ⁽¹⁵⁾, e –⁽¹⁶⁾.

The influence of pressure on the temperature of the eutectoid transformation $\gamma \rightleftharpoons \alpha + Fe_3C$ was investigated in works ^(14,15). This dependence is plotted on the diagram (Fig. 1) by a dash-dot line.

The curve $\gamma + C_r \rightleftharpoons Fe_3C$, for the same reasons, must also intersect at one point with the following three curves: the equilibrium curve $liq + C_r \rightleftharpoons Fe_3C$ and the curves of the pressure dependence of the temperatures of the eutectic transformations $liq \rightleftharpoons \gamma + Fe_3C$ and $liq \rightleftharpoons \gamma + C_r$. For calculating the equilibrium curve $liq + C_r \rightleftharpoons Fe_3C$, the necessary thermodynamic data are lacking; however, the slope of the melting curves of eutectic gray and white cast iron toward the pressure axis can be estimated with the aid of the Clapeyron equation

$$\frac{1}{T} \frac{dT}{dP} = \frac{\Delta V}{Q},$$

where T is the melting temperature, ΔV is the volume effect, and Q is the heat of fusion. The data used for this calculation are given in Table 2. In the absence of direct experimental values for the changes in volume during melting of gray and white cast iron, the values of ΔV_m were determined as follows. The volume effect of melting of eutectic white cast iron was estimated from the jump in specific volume upon melting of white cast iron on the curve of the dependence of specific volume on temperature⁽¹⁹⁾. According to⁽²⁰⁾, the increase in volume during graphitization of white cast iron is $\sim 1\%$ for each percent of carbon in the alloy, or $\sim 4.3\%$ when recalculated to the eutectic composition. From the known specific volume of white cast iron ($\sim 0.138 \text{ cm}^3/\text{g}$)⁽²⁹⁾ and its volume effect of melting, the value of ΔV_m for gray cast iron was calculated using the equality:

Table 2

Eutectic cast iron	Melting temperature T , °K	Heat of fusion Q , cal/g	Volume effect of melting $\Delta V_m = v_{tv} - v_{zh}$
Gray	1426 ⁽¹⁶⁾	46.7 ⁽¹⁷⁾ 59.0 ⁽¹⁸⁾	-0.004
White	1420 ⁽¹⁶⁾	50 ⁽¹⁷⁾	+0.002 ⁽¹⁹⁾

$$\Delta V_{m, \text{ white cast iron}} - \Delta V_{m, \text{ gray cast iron}} \approx 4.3\%;$$

dT/dP for gray cast iron is equal to -2.86°C (for $Q = 46.7 \text{ cal/g}$)⁽¹⁷⁾ and -2.26°C (for $Q = 59 \text{ cal/g}$)⁽¹⁸⁾, and for white cast iron, $+1.33^\circ\text{C}$ per 1000 kg/cm^2 . The melting curves of white and gray cast iron are plotted in Fig. 1 as thin solid lines.

The positions of the calculated equilibrium curves $(\text{C}_g \rightleftharpoons \text{Fe}_3\text{C})_\alpha$ and $(\text{C}_g \rightleftharpoons \text{Fe}_3\text{C})_\gamma$ are in satisfactory agreement with the course of the melting curves of the eutectics $\text{liq} \rightleftharpoons \gamma + \text{C}_g$ and $\text{liq} \rightleftharpoons \gamma + \text{Fe}_3\text{C}$, and with the experimentally obtained curve for the dependence of the temperature of the eutectoid transformation $\gamma \rightleftharpoons \alpha + \text{Fe}_3\text{C}$ on pressure. The equilibrium curve $(\text{C}_g \rightleftharpoons \text{Fe}_3\text{C})_\alpha$ agrees well with an analogous curve calculated earlier by Ringwood⁽²¹⁾.

As can be seen from Fig. 1, in the Fe–C system near the melting temperature of the eutectics ($\sim 1300\text{--}1400^\circ\text{K}$), at hydrostatic pressures above $\sim 2000 \text{ kg/cm}^2$, and at temperatures $\sim 1000^\circ\text{K}$ above $\sim 5000 \text{ kg/cm}^2$, the Fe–Fe₃C diagram becomes stable. It follows from this, in particular, that at any cooling rate of Fe–C melts under high pressures, carbide Fe₃C should precipitate as the stable

phase, while annealing under pressure of alloys containing graphite should lead to the transformation of graphite into cementite—the “whitening” of the alloys.

Figure 2 presents photographs of the microstructure of eutectic cast iron (4.28% C) after the following heat treatments: annealing at atmospheric pressure at a temperature of 900°C for 3 h (Fig. 2, *a, b*) and annealing at a hydrostatic pressure of 10 000 kg/cm² at the same temperatures and holding time (Fig. 2, *v, g*) with subsequent slow cooling. The initial state in both cases was gray cast iron. In Fig. 2, *a, v* (unetched sections), graphite inclusions are visible, while in Fig. 2, *b* and *g*, etching reveals the microstructure of the matrix. The individual phase constituents were identified from etchability and by measuring microhardness. After annealing at atmospheric pressure, the microstructure of gray cast iron consists of a mixture of lamellar pearlite (gray regions), ferrite (white), and graphite (black regions in Fig. 2, *b*). Annealing at high pressure led to an almost complete “whitening” of the cast iron: the number and size of graphite inclusions sharply decreased (Fig. 2, *a* and *v*) and the microstructure changed fundamentally. A large number of cementite grains appeared (white regions in Fig. 2, *g*), ferrite disappeared, and the pearlite became finer-grained. Increasing the temperature or annealing time of gray cast iron under pressure will lead to the complete disappearance of the graphite constituent.

A similar effect of pressure on the phase state of metal–carbon alloys can also be expected in the case of Ni–C and Co–C alloys. An approximate calculation, analogous to that presented above for Fe₃C, sho-

To the article by G. P. Ershov and E. G. Ponyatovskii, p. 1364

Fig. 2. Microstructure obtained after annealing gray eutectic cast iron (900°, 3 hours): **a, b**—at atmospheric pressure; **v, g**—under a pressure of 10,000 kg/cm²; **a, v**—unetched sections; **b, g**—etching in a 4% solution of nitric acid in alcohol

To the article by E. K. Keler and E. I. Kozlovskii, p. 1368

Fig. 2. Initial AMTS glass
(beginning of crystallization)

Fig. 3. Initial AMTS glass
(end of crystallization)

shows that at room temperature carbide Ni₃C becomes stable at a pressure of ~ 150 000–180 000 kg/cm², and carbide Co₃C at a pressure of ~ 20 000 kg/cm².

The authors consider it their duty to express their gratitude to Z. M. Petrova for carrying out the metallographic examination of the specimens.

Central Scientific Research
Institute of Ferrous Metallurgy
named after I. P. Bardin

Received
28 II 1963

CITED LITERATURE

1. F. D. Richardson, *J. Iron and Steel Inst.*, **175**, 33 (1953).
2. J. F. Elliott, M. Gleiser, *Thermochemistry for Steelmaking*, **1**, London, 1960.
3. L. S. Darken, R. W. Gurry, *J. Metals*, **3**, 1015 (1951).
4. *Handbook of Chemistry and Physics*, **1**, 1955–1956, p. 497.
5. R. Arnold, *Zs. angew. Phys.*, **7**, No. 9, 453 (1955).
6. O. I. Leĭpunskii, *Usp. khim.*, **8**, issue 10 (1939).
7. R. Berman, F. Simon, *Zs. Electrochem.*, **59**, No. 5, 333 (1955).
8. H. Inokuchi, M. Nakagaki, *Bull. Chem. Soc. Japan*, **32**, 65 (1959).
9. E. G. Steward, B. P. Cook, *Nature*, **185**, No. 4706, 78 (1960).
10. H. Erfling, *Ann. Phys.*, **34**, No. 2, 136 (1938–1939).
11. H. Lipson, N. J. Petch, *J. Iron and Steel Inst.*, **142**, 95 (1940).
12. B. G. Livshits, *Physical Properties of Metals and Alloys*, Moscow, 1959, p. 299.
13. Z. S. Basinski, W. Hume-Rothery, A. L. Sutton, *Proc. Roy. Soc., A* **229**, 459 (1955).
14. I. E. Hilliard, J. N. Cahn, *Progress in Very High Pressure Research*, N. Y., 1961, p. 109.
15. S. V. Radcliffe, M. Schatz, S. A. Kulin, *J. Iron and Steel Inst.*, **201**, p. 2, 143 (1963).
16. M. Hansen, K. Anderko, *Structures of Binary Alloys*, Moscow, **1**, 1962, p. 380.
17. S. Umino, *Sci. Rep. Tohoku Univ.*, **16**, 775 (1927).
18. E. Schmidt, *Zs. Metallkunde*, **7**, 164 (1915).
19. F. Sanerwald, *Zs. anorg. u. allgem. Chem.*, **155**, 51 (1929).

20. E. Piwowarsky, *Hochwertige Gußeisen*, 1958.

21. A. E. Ringwood, *Geochim. et cosmochim. acta*, **20**, 155 (1960).

Note: Figure translations are in progress. See original paper for figures.

Source: Math-Net.Ru and CyberLeninka. Machine translation. Verify with the original.